Development of Remountable Joints and Heat Removable Techniques for High-temperature Superconducting Magnets

H. Hashizume[1], S. Ito[1], N. Yanagi[2], H. Tamura[2], A. Sagara[2]

[1]Department of Quantum Science and Energy Engineering, Graduate School of Engineering, Tohoku University, Sendai, Japan

[2]National Institute for Fusion Science (NIFS), Toki, Japan

E-mail contact of main author: hidetoshi.hashizume@qse.tohoku.ac.jp

Abstract. The segment-fabrication is now being a candidate for design of superconducting helical magnet in the helical fusion reactor FFHR-d1, which adopts joint winding of high-temperature superconducting (HTS) helical coils as a primary option and the "remountable" HTS helical coil as an advanced option. This paper reports recent progress in two key technologies, mechanical joints (remountable joints) of HTS conductors and a metal porous media inserted cooling channel for the segment-fabrication. Through our research activities it was revealed that heat treatment during fabrication of the joint can reduce joint resistance and its dispersion, which can shorten fabrication process and can be applied to bent conductor joint. Also heat transfer correlations of the cooling channel was established to evaluate heat transfer performances with various cryogenic coolants based on the correlations to analyze thermal stability of joint.

1. Introduction

The "remountable" high-temperature superconducting (HTS) magnet (here "remountable" means being able to mount and demount repeatedly) has been proposed for both tokamak and helical fusion reactors [1-4], which is assembled from coil segments with mechanical joints (remountable joint) as shown in Fig. 1. The use of HTS materials can allow ohmic heating at the mechanical joints because of its high heat capacity and low refrigeration energy at relatively high operating temperature (> 20 K). This concept makes it possible to fabricate huge and complex superconducting magnet. In addition, advanced maintenance scenario can be adopted e.g. accessing inner components such as the blanket and the divertor easily by demounting the coil segments or replacing the coil segments failed by neutron irradiation or quench. Besides, concept of the joint-winding has been proposed for the helical fusion reactor, FFHR-d1, where helical coils are wound by connecting half-pitch or one-pitch conductor segments with permanent joints [5-7]. Although the segments are not demountable after completing the construction in this concept, it can provide easy fabrication of huge and complex helical coils with conventional support structures. Present conceptual design of FFHR-d1 adopts the joint-winding of the HTS coil as a primary option of its superconducting helical coil [8]. The remountable HTS magnet is also considered as an advanced option in anticipation of commercial helical fusion reactors. The aforementioned concepts collectively called the segment-fabrication of HTS magnets or the segmented HTS magnets.

There are typically two important key technologies for the segmented HTS magnets, mechanical joints of HTS conductors and local high heat removal at the joint section. This paper summarizes recent research and development (R&D) of the two key technologies. For the mechanical joints, we introduced heat treatment during fabrication of the joint and it successfully reduced joint resistance and its dispersion [9, 10]. Furthermore, we also

discussed bending characteristics of the joint for applying curved joints to the helical shaped coil [11]. For the local high heat removal, we have proposed a metal porous media inserted channel and experimentally evaluated its heat transfer performance with liquid nitrogen (LN2) [2, 12]. We newly established heat transfer correlation for the channel utilizing experimental data with water and LN2 and predicted heat transfer coefficient of various cryogenic liquid coolants needed to discuss thermal stability of joint with the cooling channel.

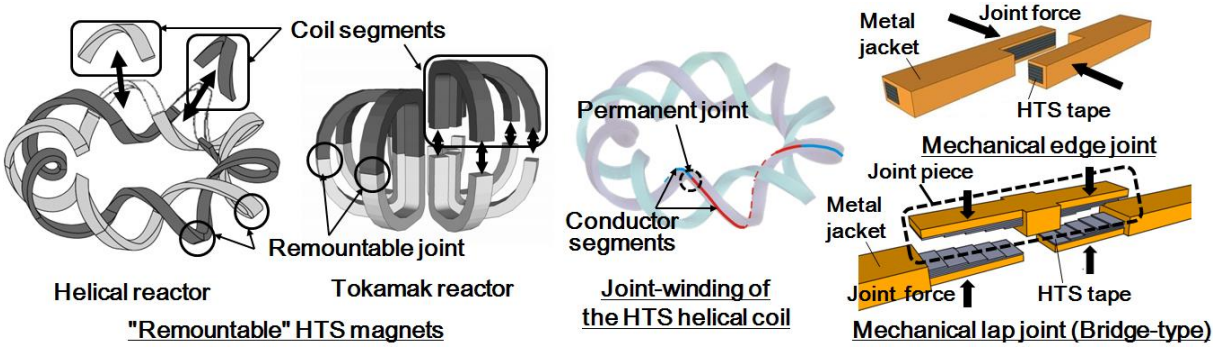

FIG. 1. Schematic illustrations of the segmented HTS magnets and the mechanical joints.

2. Remountable Joints

R&D of remountable mechanical joints is the most important issue for the remountable HTS magnet. The mechanical joints are also needed even in the joint-winding, because each joint is planned to be inspected by non-destructive testing immediately after its fabrication, then if the fabricated joint does not pass the inspection, the joint has to be demounted and a new joint will be fabricated instead of the failed joint [7]. We have proposed several types of mechanical joint: butt, edge, and lap joints [2, 7]. In these mechanical joints, joint surfaces are polished with abrasives and cleaned with ethanol, then pressed together with the indium foils inserted in-between. Indium is soft material and it can achieve relatively uniform contact pressure distribution to fill gaps on the joint surface for getting large true area of contact. Joint performance has been improved significantly for 15 years; the joint resistance decreased to be 10^{-5} times and the applied current increased to be 10^{4} times as large as those at the beginning of the R&D [2, 7]. Among the mechanical joints, we successfully developed a bridge-type mechanical lap joint of 100-kA-class HTS conductors consisting of simple stacking of Rare-Earth Barium Copper Oxide (*RE*BCO) HTS tapes embedded in copper and stainless steel jackets. The joint achieved a joint resistance of 1.8 nΩ at 100 kA, 4.2 K [6, 7, 13]. If we achieve an averaged joint resistance of about 2 nΩ at all joint section in the segmented magnet, the electric power required to run the cryoplant is sufficiently lower than that for low-temperature superconducting magnet without joint section [9]. Although we experimentally demonstrated low joint resistance with a bridge-type mechanical lap joint of the 100-kA-class HTS conductors, the fabricated joint had straight geometry. Furthermore the joint resistance obtained with large-scale conductor joint was still larger than predicted value based on small-scale conductor joint and dispersed widely due to non-uniform contact pressure distribution on the joint surfaces [7]. Based on the aforementioned situation, we newly developed new fabrication method of the joint with heat treatment [9, 10] and evaluated bending characteristics [11] of the bridge-type mechanical lap joint.

2.1.Joint resistance reduction by heat treatment

The real contact area should increase inversely proportional to hardness of contact material according to contact theory [14]. The indium inserted between joint surfaces has a low

melting temperature of 156.6 °C and therefore it soften very much even at ~100 °C. Fig. 2 (a) shows the experimental set-up for the heat treatment where the joint pressure can be kept during the heat treatment. Fig. 2 (b) shows joint resistivity (product of joint resistance and joint area) at 77 K for mechanical lap joint of single *RE*BCO tapes as a function of heating temperature during the fabrication. The joint resistivity can be reduced by 60% with the heat treatment and bake-out processes [9, 10]. We also applied the heat treatment to a bridge-type mechanical lap joint of *RE*BCO conductors with three-rows and one-layer. The joint resistivity was reduced from 25 pΩm^2 to 8 pΩm^2 after heating. This means the heat treatment is promising to be applied to large-scale conductor joints, which possibly show relatively large joint resistance due to variation in quality.

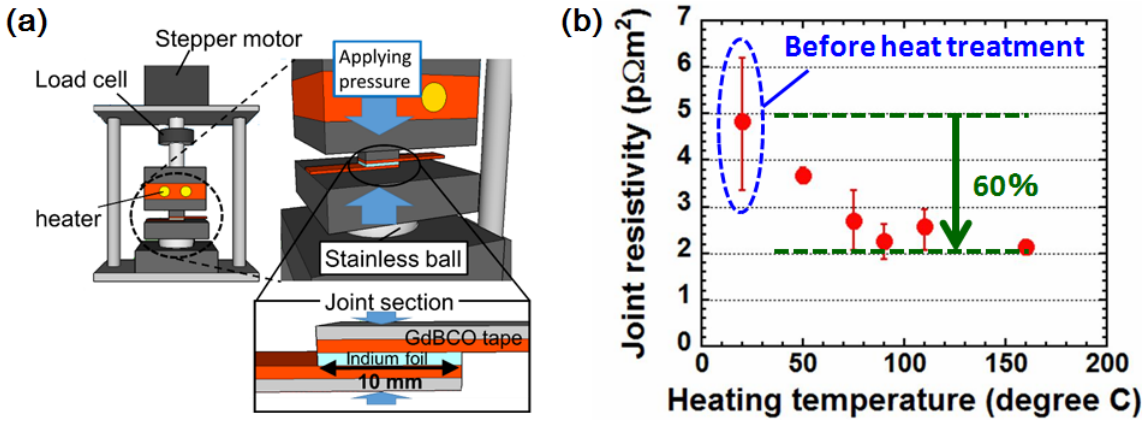

FIG. 2. Joint resistance reduction by the heat treatment during fabrication process of the joint [10]: (a) Experimental set-up, (b) Joint resistivity as a function of heating temperature.

2.2.Bending characteristics

We evaluated the bending characteristics of a bridge-type mechanical lap joint of 4-mm-wide *RE*BCO tapes with indium foils inserted between joint surfaces: joint resistivity and critical current as a function of bending strain (tensile strain induced by bending at the joint) applied at room temperature [11]. Fig. 3 (a) shows an example of the results of the bending tests for joint samples with a joint length of 10 mm. The experimental results showed that critical bending strain where joint resistance starts to increase becomes higher with decreased joint resistivity and increased joint length. Irreversible tensile strain of the present *RE*BCO tapes was reported to be about 0.6% [15] and the critical bending strain for the joint resistivity was larger than the irreversible strain in the sample with a joint length of 10 mm and a joint resistivity of 4.26 pΩm^2 shown in Fig. 3 (a) at least. In the latest design of joint-winding of the HTS helical coils, the joint length is 25 mm for each layer of *RE*BCO tape [7] and we also plan to apply the heat treatment for its fabrication, which implies that joint has sufficient strength against bending. Fig. 3 (b) shows curvature radius of the helical coils for FFHR-d1A. The minimum curvature radius of neutral plane of the helical coil is 5.92 m and the thickness of the helical coil is 930 mm. Therefore, the minimum radius of inner most conductors is about 5.45 m. The thickness of the *RE*BCO tape stacks in an HTS conductor is assumed to be 5 mm here, and then we obtain 0.046% bending strain in the stacks. The bending strain is sufficiently lower than the irreversible strain and critical bending strain for joint resistivity. Structural analysis of the helical coil for FFHR-d1A [7] also shows a tensile strain of 0.145% induced by electromagnetic forces. The total tensile strain is 0.191%, which is still lower than the irreversible strain. The above discussion indicates that we can take fabrication procedure "joining-then-bending" if we adopt curved joint to the joint-winding.

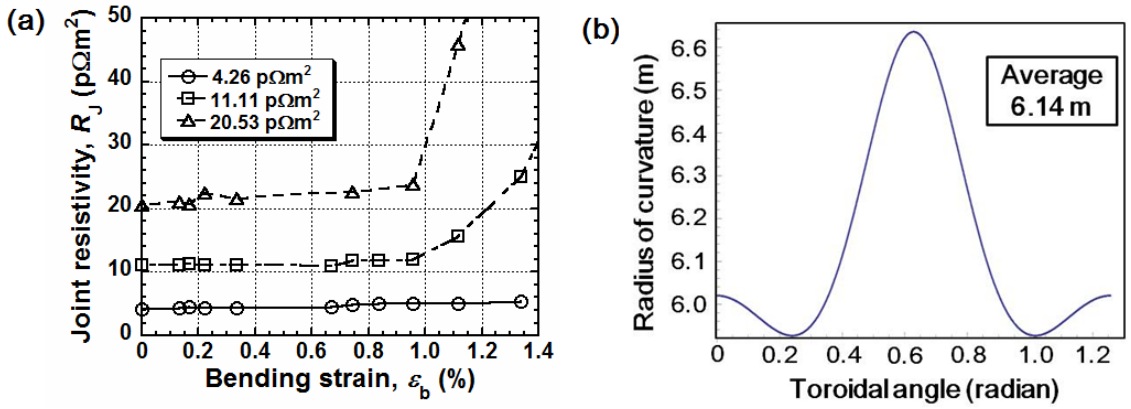

FIG. 3. Bending characteristics of a bridge-type mechanical lap joint test and radius of curvature for the helical coils: (a) Joint resistivity as a function of bending strain and initial joint resistivity [11], and (b) The radius of curvature of the helical coil along the toroidal angle in the case of FFHR-d1A.

3. Heat Removal Techniques

From a view-point of the refrigeration energy, the mean value of joint resistance at all joint section is important to judge the design feasibility. This implies relatively higher joint resistance at each joint section is allowed unless the mean joint resistance is larger than the acceptable value. However, the acceptable joint resistance at each joint section is also determined by thermal stability, which is affected by cooling performance in the joint region. Especially, the joint resistance possibly becomes higher in the remountable magnet assembled from coil segments due to electromagnetic forces and difficulty of joining the coil segments consisting of several hundreds of HTS conductor all at once. A cooling channel with metal porous media and cryogenic coolants has been proposed for the situation [2, 12]. Some studies [12, 16] reported cooling performance based on experiments using metal-particle sintered porous media with different coolants, water and LN2. Although they showed that the channels could remove high heat flux using latent heat of the coolants, the heat transfer correlation to design cooling system of the magnet has not been discussed yet in terms of wall superheat and heat flux. Therefore, in this study, a new correlation for forced convection, nucleate boiling and departure from nucleate boiling (DNB) point for metal-particle sintered porous media inserted into cooling channel is discussed based on experimental data and existing correlations for various cooling channels.

3.1. Heat transfer correlations for metal-particle sintered porous media inserted into a cooling channel

Boiling curve of water and LN2 experimentally obtained in previous studies [12, 16] are used for establishing the heat transfer correlations, in which bronze-particle sintered porous media were inserted into cooling channels. We additionally evaluated the boiling curve of LN2 flowing through the bronze porous media as a function of particle diameter, d, flow rate, G, and inlet degree of subcooling of LN2, ΔT_{sub}, as missing data using the same experimental set-up as described in [12]. Fig. 4 (a) shows an example of boiling curve (relationship between wall superheat, ΔT_{sat}, and heat flux, q) obtained in the present study. Heat transfer conditions can be categorized into the following three regions; "forced convection region", "forced convection nucleate boiling region", and "mixed region of nucleate and film boiling region".

We modified Achenbach's equation [17] for the correlation of forced convection heat transfer in a non-sintered porous channel based on the data for water [16] as the following equation,

$$Nu_d = C\left(1 - \frac{1}{D/d}\right) Re_d^{0.61} Pr^{1/3} \left(\frac{\mu_{bulk}}{\mu_w}\right)^{0.14} \left(\frac{\alpha_{eff}}{\alpha_S}\right)^{0.65} \quad (1)$$

where Nu_d, Re_d, Pr, D, μ_w, μ_{bulk}, α_S and α_{eff} are Nusselt number based on particle diameter, Reynolds number based on the particle diameter, Prandtl number, pipe diameter (hydraulic diameter), viscosity at wall temperature, viscosity at bulk temperature, thermal diffusivity of the porous medium, and effective thermal diffusivity of the porous medium taking volume fraction of solid and fluid, respectively. C is constant value related to thermal resistance between heat transfer surface and the porous medium: $C = 0.6$ for the porous medium mechanically contacted to the surface and $C = 0.9$ for the porous medium sinter-bonded to the surface. Fig. 4 (b) shows comparisons between heat fluxes derived by Eq. (1) and obtained by the experiments with water and LN2 in forced convection region. The modified equation has accuracy of range of ±40%.

Generally, heat flux by forced convection nucleate boiling heat transfer is expressed as $q = h_{conv}\Delta T_{bulk} + h_{boil}\Delta T_{sat}$ where h_{conv} and h_{boil} are heat transfer coefficients for forced convection and nucleate boiling, and ΔT_{bulk} is wall-to-fluid temperature difference, respectively. We assumed that the effect of forced convection decreases with increasing that of nucleate boiling. Furthermore, we modified Chen's equation [18] for pool boiling in a smooth tube as nucleate boiling heat transfer, assuming that the influence of wall-superheat on the heat flux halves because nucleate boiling occurs both on heat transfer surface and inside the porous medium due to thermal conduction. The modified equations for forced convection nucleate boiling are,

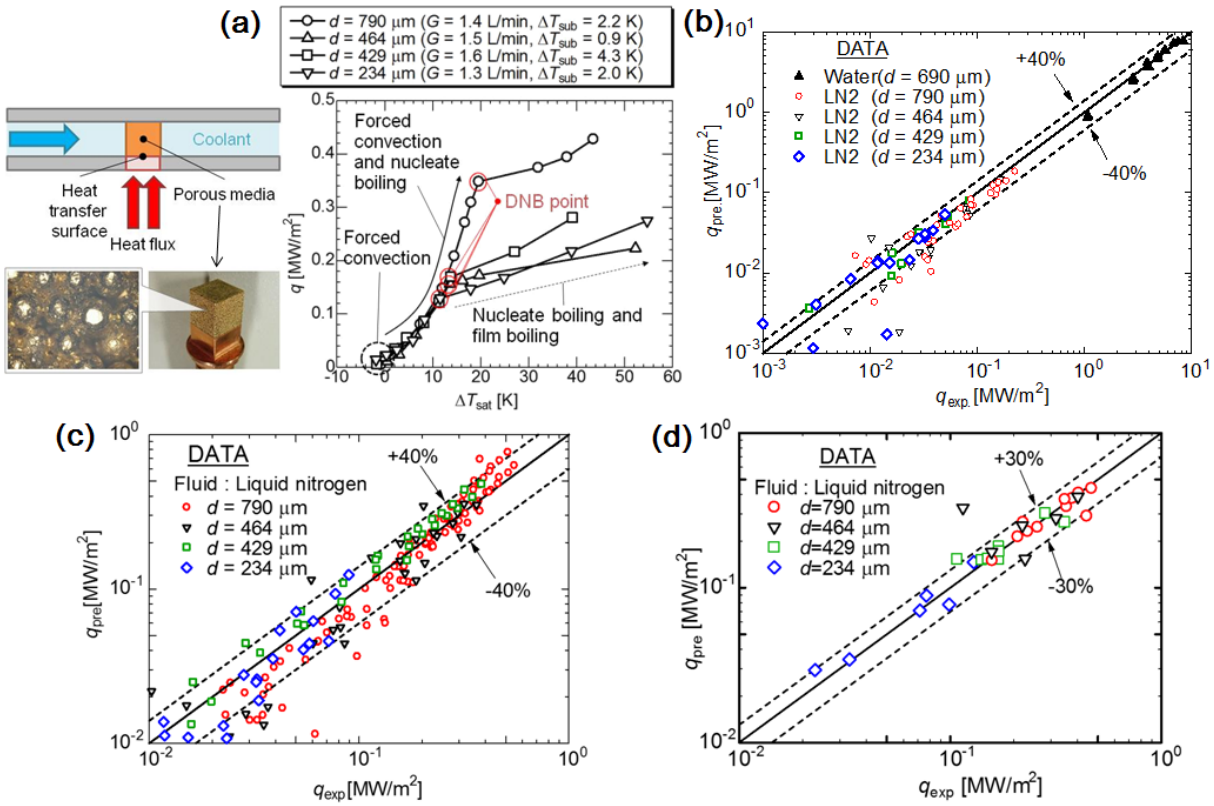

FIG. 4. An example of experimentally evaluated boiling curve and comparisons between heat fluxes derived by the correlations and obtained by the experiments: (a) Experimentally evaluated boiling curve, (b) Comparison in forced convection region, (c) Comparison in forced convection nucleate boiling region, and (d) Comparison in DNB point.

$$
\begin{aligned}
q &= \left(1 - \frac{\Delta T_{\mathrm{sat,DNB}}}{2}\right) h_{\mathrm{conv}} \Delta T_{\mathrm{bulk}} + h_{\mathrm{boil}} \left(\frac{\Delta T_{\mathrm{sat}}}{2}\right), \\
h_{\mathrm{boil}} &= 0.00122 \left(\frac{k_{\mathrm{L}}^{0.79} C_{p\mathrm{L}}^{0.45} \rho_{\mathrm{L}}^{0.49}}{\sigma^{0.5} \mu_{\mathrm{L}}^{0.29} h_{\mathrm{LG}}^{0.24} \rho_{\mathrm{G}}^{0.24}}\right) \left(\frac{\Delta T_{\mathrm{sat}}}{2}\right)^{0.24} \Delta P_{\mathrm{sat}}^{0.75} S, \\
S &= \frac{1}{1 + 2.53 \times 10^{-6} Re_D^{1.17}}, \qquad Re_D = \frac{(1-\chi)\rho_{\mathrm{L}} u D}{\mu_{\mathrm{L}}}
\end{aligned}
\tag{2}
$$

where $\Delta T_{\mathrm{sat,DNB}}$, k_{L}, $C_{p\mathrm{L}}$, σ, μ_{L}, h_{LG}, ρ_{L}, ρ_{G}, ΔP_{sat}, Re_D, u and χ are wall-superheat at DNB point, thermal conductivity of liquid, isobaric specific heat of liquid, surface tension, viscosity of liquid, evaporative latent heat, density of liquid, density of gas, difference in vapor pressure corresponding to ΔT_{sat}, Reynolds number based on pipe diameter (hydraulic diameter), mean velocity and vapor quality, respectively. The modified equations shown in Eq. (2) have accuracy of range of ±40% as shown in Fig. 4 (c).

For predicting heat flux at DNB point, q_{DNB}, we modified Katto's and Bowers' equations [19, 20] for convection boiling for smooth tube. The modified equations are obtained as follows, assuming that the porous channel is expressed to have a lot of micro-parallel-channel as in "channel model" in the modified equation.

$$
\begin{aligned}
&\frac{q_{\mathrm{DNB}}}{m h_{\mathrm{LG}}} = 0.0186 \left(\frac{\rho_{\mathrm{G}}}{\rho_{\mathrm{L}}}\right)^{0.133} We^{0.0976} \left(\frac{L}{d_{\mathrm{e}}}\right)^{-0.259}, \; m = \frac{\rho_{\mathrm{L}} G}{A'}, \\
&A' = \left(N \times \frac{\pi d_{\mathrm{e}}^2}{4}\right), \; N = \frac{D^2}{\pi d_{\mathrm{e}}^2 / 4} \times \varepsilon, \qquad \mathrm{d_e} = \frac{2}{3} \frac{\varepsilon d}{1 - \varepsilon}
\end{aligned}
\tag{3}
$$

where m, We, L, d_{e}, A', N, ε are mass flow rate, Weber number, heated length of heat sink channel, diameter of micro channel, total cross sectional area of micro channels, the number of micro channel and porosity of porous medium, respectively. The modified equation has accuracy of range of ±30% as shown in Fig. 4 (d).

3.2.Prediction of heat transfer performance for various cryogenic coolants

Cooling performance of liquid helium (LHe), liquid hydrogen (LH2) and liquid neon (LNe) in a channel with bronze-particle sintered porous media was predicted by using the three correlation equations. Fig. 5 (a) shows relationship between volume flow rate and pressure drop of each coolant flowing thorough a 12-mm cube of bronze-particle sintered porous medium with d = 790 μm and ε = 26%, which is derived by Ergun's equation [21] estimating pressure drop in porous channels. Open and closed symbols correspond to pomp powers of 0.1 W and 1 W, respectively. Fig. 5 (b), (c) and (d) show boiling curves derived by the correlation equations. At the constant pump power and each coolant's saturated temperature, LH2 and LNe show almost the same heat transfer coefficient and DNB point. The DNB point for LH2 and LNe is about 10 times larger than that for LHe. LNe is the best from the viewpoint of chemical stability whereas LH2 is the best from a view point of cost.

4. Conclusions

This study addresses development of mechanical joints and a heat removable technique for the segmented HTS magnets. We carried out (i) Optimizing fabrication procedure of mechanical joints, and (ii) Analyzing heat transfer performance of metal porous media inserted channel to be applied to thermal analysis of joint. The developments and discussion will be taken into account in design of the segmented HTS magnet.

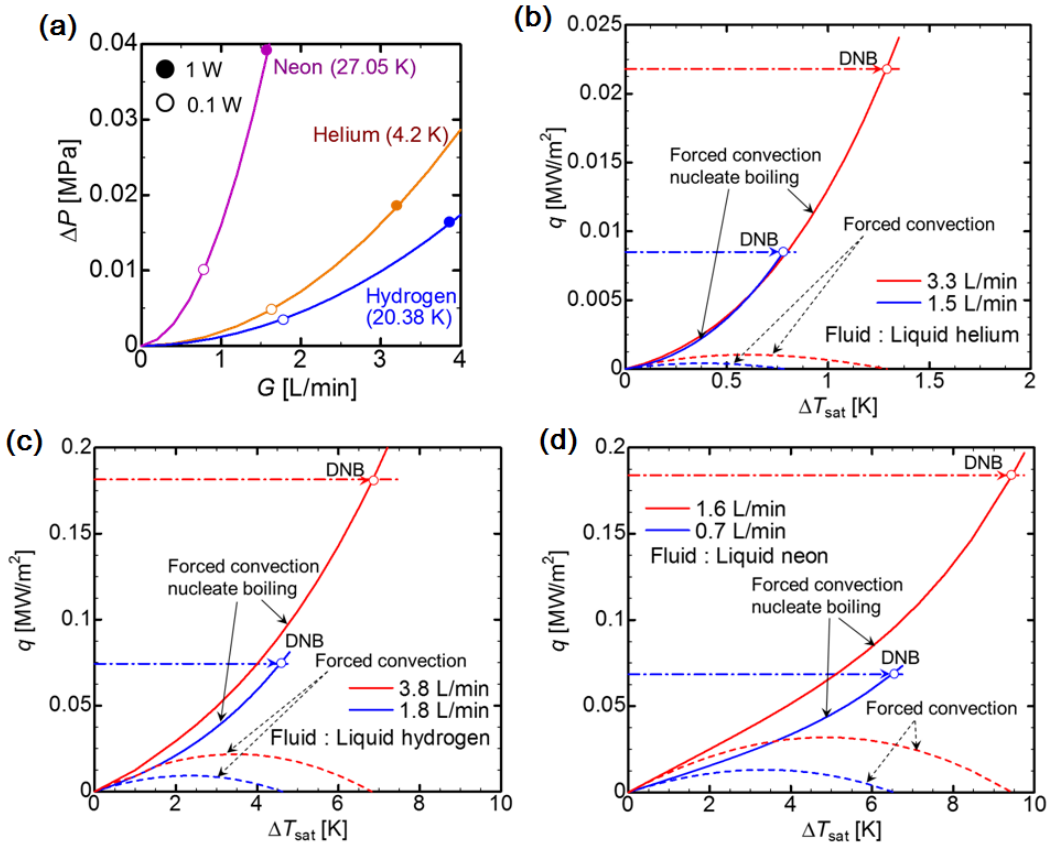

FIG. 5. Predicted heat transfer characteristics for various cryogenic coolants in a 12-mm cube of bronze-particle sintered porous medium with a particle diameter of 790 μm and a porosity of 26%: (a) Volume flow rate vs pressure drop, (b) boiling curve for liquid helium, (c) boiling curve for liquid hydrogen, and (c) boiling curve for liquid neon.

Acknowledgement

This work was supported in part by the Japan Society for the Promotion of Science (JSPS) Grant-in-Aid for Scientific Research (S) under Grant 26220913; by the JSPS Grant-in-Aid for Scientific Research (C) under Grant 26420849; by the NIFS Collaboration Research program (NIFS16KECF01).

References

[1] HASHIZUME, H., et al., "Advanced fusion reactor design using remountable HTc SC magnet", J. Plasma Fusion Res. Ser., **5** (2002) pp. 532–536.

[2] HASHIZUME, H., ITO, S., "Design prospect of remountable high-temperature superconducting magnet", Fusion Eng. Des., **89** (2014) pp. 2241–2245.

[3] BROMBERG, L., et al., "Options for the use of high temperature superconductor in tokamak fusion reactor designs", Fusion Eng. Des., **54** (2001) pp. 167–180.

[4] HARTWIG, Z., et al., "An initial study of demountable high-temperature superconducting toroidal magnets for the Vulcan tokamak conceptual design", Fusion Eng. Des., **87** (2012) pp. 201–214.

[5] YANAGI, N., et al., “Design progress on the high-temperature superconducting coil option for the heliotron-type fusion energy reactor FFHR”, Fusion Sci. Technol., **60** (2011) pp. 648–652.

[6] YANAGI, N., et al., “Design and development of high-temperature superconducting magnet system with joint-winding for the helical fusion reactor”, Nucl. Fusion, **55** (2015) 053021.

[7] ITO, S., et al., “Mechanical and Electrical Characteristics of a Bridge-type Mechanical Lap Joint of HTS STARS Conductors”, IEEE Trans. Appl. Supercond., **26** (2016) 4202405.

[8] SAGARA, A., et al., “Helical reactor design FFHR-d1 and c1 for steady-state DEMO”, Fusion Eng. Des., **89** (2014) pp. 2114–2120.

[9] NISHIO, T., ITO, S., YUSA, N., HASHIZUME, H., “Reducing joint resistance by heat treatment during fabrication of a mechanical joint of high-temperature superconducting conductors”, IEEE Trans. Appl. Supercond., **26** (2016) 4800505.

[10] NISHIO, T., ITO, S., HASHIZUME, H., “Heating and loading process improvement for indium inserted mechanical lap joint of REBCO tapes”, IEEE Trans. Appl. Supercond. (Submitted).

[11] ITO, S., NISHIO, T., HASHIZUME, H., “Bending Characteristic of a Bridge-type Mechanical Lap Joint of REBCO Tapes”, IEEE Trans. Appl. Supercond. (Submitted).

[12] TANNO, Y., ITO, S., HASHIZUME, H., “Characteristic Evaluation of Cooling Technique using Liquid Nitrogen and Metal Porous Media”, Advances in Cryogenic Eng., AIP conf. Proc. **1573** (2014) pp. 597–604.

[13] ITO, S., et al., “Bridge-Type Mechanical Lap Joint of a 100 kA-Class HTS Conductor having Stacks of GdBCO Tapes”, Plasma Fusion Res., **9** (2014) 3405086.

[14] TABOR, D., “The hardness of metals”, Oxford University Press (1951) pp. 141–154.

[15] SONG, H., et al., “2G HTS coil technology development at SuperPower”, IEEE Trans. Appl. Supercond., **23** (2013) 4600806.

[16] YUKI, K., MATSUI, A., HASHIZUME, H. SUZUKI, K., “Proposal of a Micro/Mini Cooling Device using Fins-installed Porous Media for High Heat Flux Removal exceeding 1000W/cm^2”, Proceedings of Micro/Nanoscale Heat Transfer International Conference 2009, Dec. 18–21 2009, Shanghai, China, MNHMT2009-18318.

[17] ACHENBACH, E., “Heat and Flow Characteristics of Packed Beds”, Exp. Therm. Fluid Sci., **10** (1995) pp. 17–27.

[18] CHEN J.C., “Correlation for Boiling Heat Transfer to Saturated Fluids in Convective Flow”, Ind. Eng. Chem. Process Des. Dev., **5** (1996) pp 322–329.

[19] KATTO, Y., “General Features of CHF Forced Convection Boiling in Uniformly Heated Rectangular Channels”, Int. J. Mass Heat Transfer, **24** (1981) pp. 1413–1419.

[20] BOWERS, M.B., MUDAWAR, I., “High flux boiling in low flow rate, low pressure drop mini-channel and micro-channel heat sinks”, Int. J. Mass Heat Transfer, **37** (1994) pp. 321–332.

[21] ERGUN, S., “Fluid flow through packed columns”, Chem. Eng. Prog., **48** (1952) pp. 89–94.